ORIGINAL ARTICLE

Preheating of Gelatin Improves its Printability with Transglutaminase in Direct Ink Writing 3D Printing

Justin Jia Yao Tan[1,2†], Cheng Pau Lee[1,2†], Michinao Hashimoto[1,2*]

[1]Pillar of Engineering Product Development, Singapore University of Technology and Design, 8 Somapah Road, Singapore 487372, Singapore

[2]SUTD-MIT International Design Centre, Singapore University of Technology and Design, 8 Somapah Road, Singapore 487372, Singapore

†These authors contributed equally to this paper.

Abstract: Gelatin and transglutaminase (TG) ink is increasingly popular in direct ink writing three-dimensional (3D) printing of cellular scaffolds and edible materials. The use of enzymes to crosslink gelatin chains removes the needs for toxic crosslinkers and bypasses undesired side reactions due to the specificity of the enzymes. However, their application in 3D printing remains challenging primarily due to the rapid crosslinking that leads to the short duration of printable time. In this work, we propose the use of gelatin preheated for 7 days to extend the duration of the printing time of the gelatin ink. We first determined the stiffness of freshly prepared gelatin (FG) and preheated gelatin (PG) (5 – 20% w/w) containing 5% w/w TG. We selected gelatin hydrogels made from 7.5% w/w FG and 10% w/w PG that yielded similar stiffness for subsequent studies to determine the duration of the printable time. PG inks exhibited longer time required for gelation and a smaller increase in viscosity with time than FG inks of similar stiffness. Our study suggested the advantage to preheat gelatin to enhance the printability of the ink, which is essential for extrusion-based bioprinting and food printing.

Keywords: Gelatin, Transglutaminase, Direct ink writing, Extrusion-based 3D printing, Printability, Preheating

***Corresponding Author**: Michinao Hashimoto, Pillar of Engineering Product Development, Singapore University of Technology and Design, 8 Somapah Road, Singapore 487372, Singapore; hashimoto@sutd.edu.sg

Received: April 06, 2020; ***Accepted:*** June 07, 2020; ***Published Online*:** September 08, 2020

Citation: Tan JJY, Lee CP, Hashimoto M, Preheating of Gelatin Improves its Printability with Transglutaminase in Direct Ink Writing 3D Printing, *Int J Bioprint*, 6(4): 296. DOI: 10.18063/ijb.v6i4.296.

1 Introduction

This paper discusses the effects of preheating gelatin on its printability through direct ink writing (DIW) three-dimensional (3D) printing. Recent developments in 3D printing and additive manufacturing have extended into the fields of tissue engineering[1,2], sensing[3], and food engineering[4,5]. In the field of tissue engineering, anatomical replicas of human organs such as skin, heart, lung, kidney, and liver have been printed. These 3D printed organs have been shown to express the characteristics of tissue markers and spatial orientations as native human organs[1]. Strategies have been developed to improve the resolution, shape fidelity, and complexity of these 3D printed organs. Examples include delaying cell sedimentation within the bioink through the addition of non-adhesive polymers or weakly crosslinked hydrogels[2]. In sensing, 3D printing has been used to fabricate multi-material, multifunctional stretchable electronic devices, ranging from wearable electronics, energy

harvesting devices, to prosthetic bionic skins[3]. The adoption of 3D printing technology offers multiple advantages over traditional techniques to fabricate scaffolds, including uniformity and reproducibility in manufacturing, reduction of user error, and precise control over scaffold pore size, connectivity, and geometry[6]. Among the materials used in extrusion-based printing, natural biopolymers such as collagen, gelatin, and chitosan are promising candidates for bioprinting and food printing due to their excellent biocompatibility and abundance of cell recognition sites[7,8]. In addition, natural biopolymers such as gelatin are inexpensive to fabricate, and they can be synthesized with relative ease[9]. Essential physical properties (such as stiffness and water content) can be altered to obtain similar elastic modulus of native tissues such as skeletal muscle, which was previously reported to be within the range of 10 – 50 kPa[10]. Finally, gelatin is a generally edible material and can eventually be used for food printing as a ready-to-eat product without the need for post-processing. These properties make the gelatin as a desirable candidate for the application in 3D printing.

3D printing of gelatin would require adequate control over the physical properties of the gelatin inks. The melting point of gelatin is 30 – 37°C, depending on their bloom strength, pH, and concentration[11]; gelatin is unable to hold/retain its structure and would melt at physiological temperature. Permanent peptide bonds need to be formed between amino acids to ensure the integrity of the structure in a liquid medium and at physiological temperature. Among the most employed techniques to achieve permanent crosslinking are photocrosslinking and enzymatic crosslinking. Photocrosslinking between methacryloyl groups in Gelatin-Methacryloyl happens relatively fast (in the order of seconds), which rapidly confers structural stability to the printed scaffold[12]. Enzymatic crosslinking (i.e., using transglutaminase [TG]), on the other hand, takes place relatively slower (in the order of minutes) than photocrosslinking. Although slower, TG has been widely used as a meat glue to mediate the crosslinking of gelatin; the crosslinked product remains edible, which is the requirement for 3D food printing. In addition, enzymatic crosslinking does not produce free radicals and uncrosslinked monomers derived from photocrosslinking reactions that might adversely affect the cellular conditions. Both photocrosslinking and enzymatic crosslinking are permanent and confer mechanical strength to the crosslinked gelatin chains required for 3D printing. TG is often added to gelatin to facilitate the formation of the peptide bond between the γ-carbonyl group of glutamine residue and the ε-amino group of a lysine residue within the gelatin[9]. The formation of peptide bonds stabilizes the structure of the printed scaffold and improves its structural integrity. This enzymatic crosslinking is favored among other available methods of crosslinking (such as chemical crosslinking) due to the low occurrence of side reactions (due to substrate specificity) and no cellular toxicity of the enzymes. The use of enzymes also eliminates the need for specialized equipment and other photo-sensitive additives that may be toxic in nature[9].

DIW 3D printing has been widely demonstrated in 3D printing for polymers, foods, hydrogels[13, 14]. Polymers such as polyvinyl alcohol were 3D printed to serve as coating layers for controlling the drug release of active ingredients[15]. For the application in food printing, rheology-modified food inks have been printed using a DIW 3D printer to model complex 3D shapes without temperature control[5]. Potato starch-containing anthocyanin and lemon juice was 3D printed as a two-part gel system exhibited time-dependent color change in response to the diffusion of hydrogen ions from the lemon juice layer into the anthocyanin layer[16]. Such 3D-printable hydrogels included photo-curable polyethylene glycol acrylate, poly(2,6-dimethyl-1,4-phenylene oxide) acrylate, gelatin-methacrylate, and hyaluronan-methacrylate[17-19]. In addition, gelation can be triggered by printing a hydrogel-forming polymer solution into a bath of the reactive substance. It was reported that alginate printed into calcium solution using this method has yielded complex cell-laden 3D structures maintaining cell viability[20]. DIW of these hydrogel-forming polymers offers a

rapid and relatively cell-friendly method for the making of cellular scaffolds[21]. In DIW 3D printing, a continuous ink filament is extruded through a nozzle onto a stationary substrate from a microscale syringe tip driven by either pneumatic pressure or mechanical force[22]. Although gelatin and TG ink is an ideal material for 3D printing, its application in 3D printing remains challenging because of the difficulty to control the physical and rheological properties of the ink.

In particular, 3D printing with gelatin and TG is limited by the rate of enzymatic crosslinking; the rapid crosslinking influenced the gelation time of the ink[9]. The fast crosslinking would result in the rapid gelation of the liquid gelatin ink. The gelation of the ink increases its viscosity and results in clumps in ink. These clumps diminish the quality of the printed structures and clog the nozzle during printing. It was reported that printing was only possible for approximately 3 min at 37°C before the crosslinking reaction prevents ink flow due to blockage[9]. Future optimization was therefore required to identify other approaches to extend the printing time.

To enhance the usability of the freshly prepared gelatin (which we term FG) inks crosslinked with TG in 3D printing, we propose to use preheated gelatin (which we term PG) inks to extend the printing time. We first evaluated the stiffness of hydrogels prepared from FG and PG crosslinked with TG. Envisaging applications in bioprinting, we identified the concentrations of gelatin and TG in ink. We then 3D printed grid patterns for FG and PG possessing similar stiffness and assessed their printability, gelation, and viscosity profiles. Finally, we incubated hydrogels in phosphate-buffered saline (PBS) to determine their swelling profiles. Our experiments suggested that hydrogels prepared from PG (10% w/w) offered approximately 4 to 10 times longer printing time. Finally, we found that PG inks exhibited greater shrinkage at low concentrations (i.e., 7.5% and 10% w/w) and greater swelling at high concentrations (i.e., 20% w/w) than FG inks of the same concentrations. The shrinkage of PG may allow reducing the size of the printed models by post-processing. Our study suggested the preheating of gelatin as a simple way to influence the printability and the volume change of the ink. The insights gained in this study shall be applicable for applications in 3D printing to extend the printing time of the gelatin and TG ink to fabricate large cellular scaffolds or intricate structures for bioprinting and food printing.

2 Results and discussion

2.1 Justification of approach

Several approaches are possible to extend the duration of the printable time for the gelatin inks crosslinked with TG, including (1) lowering the concentration of gelatin, (2) lowering the concentration of TG, and (3) altering printing temperature. In this paper, we excluded the alteration of the concentration of the materials from our possible approaches to achieve the goal. It was previously reported that changing gelatin concentration had a small effect on the gelation time of the gelatin and TG ink[9]. Lowering the TG concentration to increase the duration of printing was reported to lower the overall hydrogel stiffness greatly[9]; the resulting hydrogels possessed poor stability in aqueous environments due to the reduced degrees in crosslinking between gelatin chains. The uncrosslinked gelatin chains would be washed out in the surrounding aqueous environment, destabilizing the printed gelatin structure. Because of this reason, we fixed the concentration of TG as 5% w/w throughout the current study. Alteration of the printing temperature would influence the viscosity of the ink and the stability of TG, and we did not employ that approach to achieve extended printable time.

We selected to investigate the effect of preheating of gelatin. Gelatin absorbs water and swells in liquid media[23]. Preheating of gelatin has been reported to reduce its extent of swelling[24]. When the gelatin is preheated, the internal hydrogen bonds responsible for holding the triple helical structure of gelatin are broken. A previous study reported that the unfolding of the triple helical structure exposes more hydrophobic amino acids, increasing the surface hydrophobicity of the gelatin[25]. However, when gelatin undergoes

chemical crosslinking, the formation of a rigid network reduces the extent of swelling in the resulting hydrogel[26]. In this study, we investigated the effect of swelling of FG and PG crosslinked with TG.

2.2 Evaluation of hydrogel stiffness

Initially, stiffness of hydrogels prepared from FG and PG crosslinked with TG (5% w/w) was investigated. Stiffness is an essential mechano-physical property that influences cell growth and function[27]. We intended to show that PG would be able to confer better printability than FG for the hydrogels yielding similar stiffness. We have chosen hydrogels yielding an estimated elastic modulus of 10 kPa, which is tissue-like stiffness deemed suitable for the culture of many cell types, including myoblasts, human primary keratinocytes, and human embryonic stem cells[28-30]. Amplitude sweep tests were conducted for FG and PG with the concentrations ranging from 5 to 20% w/w while keeping TG concentration at 5% w/w. We use the following nomenclature to describe the composition of FG and PG throughout the current study. For instance, FG10 indicates that the ink contained 10% w/w FG and 5% w/w TG, while PG10 indicates that the ink contained 10% w/w PG and 5% w/w TG. The hydrogel stiffness was determined by its elastic modulus, which was estimated from the storage modulus obtained from the viscoelastic region of the flow diagrams, as reported.[31] The estimated elastic modulus of both FG and PG hydrogels increased with gelatin concentrations. Exposure of gelatin to high temperatures for extended periods resulted in the thermal hydrolysis of the polypeptide chains. Thermal hydrolysis caused a decrease in the gel rigidity (i.e., gel strength)[32]. The stiffness of hydrogels of FG7.5 was similar to PG10, both of which yielded an estimated elastic modulus of approximately 10 kPa (**Figure 1**). We chose these two hydrogel compositions for our subsequent work because they yielded a tissue-like stiffness which deemed suitable for the culture of many cell types. Highly stiff substrates were not favored for cell cultures, as multiple studies have shown that cells preferentially grow and differentiate on soft, tissue-like substrates[33-35]. We also included FG10 for our later study as a control for preheating; FG10 and PG10 contained the same gelatin concentration, and the observed differences, if any, shall be attributed to the consequences of preheating. After identifying suitable inks (that is, FG7.5, FG10, and PG10), we proceeded to assess their printability.

2.3 3D printing of gelatin and TG inks and printability characterization

The printability of the inks was assessed at selected time points using the printability value (*Pr*)[36]. *Pr* indicated the degree of gelation of the extruded filament at the respective time points[36]. Three states of gelation were considered for the printed inks: Under-gelation, proper-gelation, and over-gelation. Under-gelation would yield obvious chamfers in the printed grids due to the fusion of the subsequent two layers of the interconnected filaments ($Pr < 1$). During proper-gelation, the interconnected filaments would demonstrate a perfect square shape or close to a square with regular edges ($Pr = 1$). Over-gelation, however, led to the formation of irregularly printed and interconnected filaments ($Pr > 1$). The larger values of *Pr* indicated the higher degree of gelation while the smaller *Pr* indicated the lower degree of gelation. We set the acceptable range of *Pr* to be 0.9 – 1.1, as reported previously with 3D printed hydrogel constructs[36].

FG7.5, FG10, and PG10 were printed in a grid pattern on a glass surface at 3 min, 5 min, 10 min, and every 5 min after that. The printing was stopped when the inks became clumpy or when the ink could not be extruded at the maximum pressure of the dispenser. The Hagen-Poiseuille equation suggested that the volumetric flow rate was inversely proportional to the viscosity of fluids[37]. Continuous increase in the viscosity required compensation by the increase in the applied pressure. We observed that extruding FG inks were more challenging than PG due to the rapid increase in the viscosity (**Figure 2A** and **2B**).

Under-gelation was observed for FG7.5 at 3 min but not for FG10 (**Figure 2A**). The duration

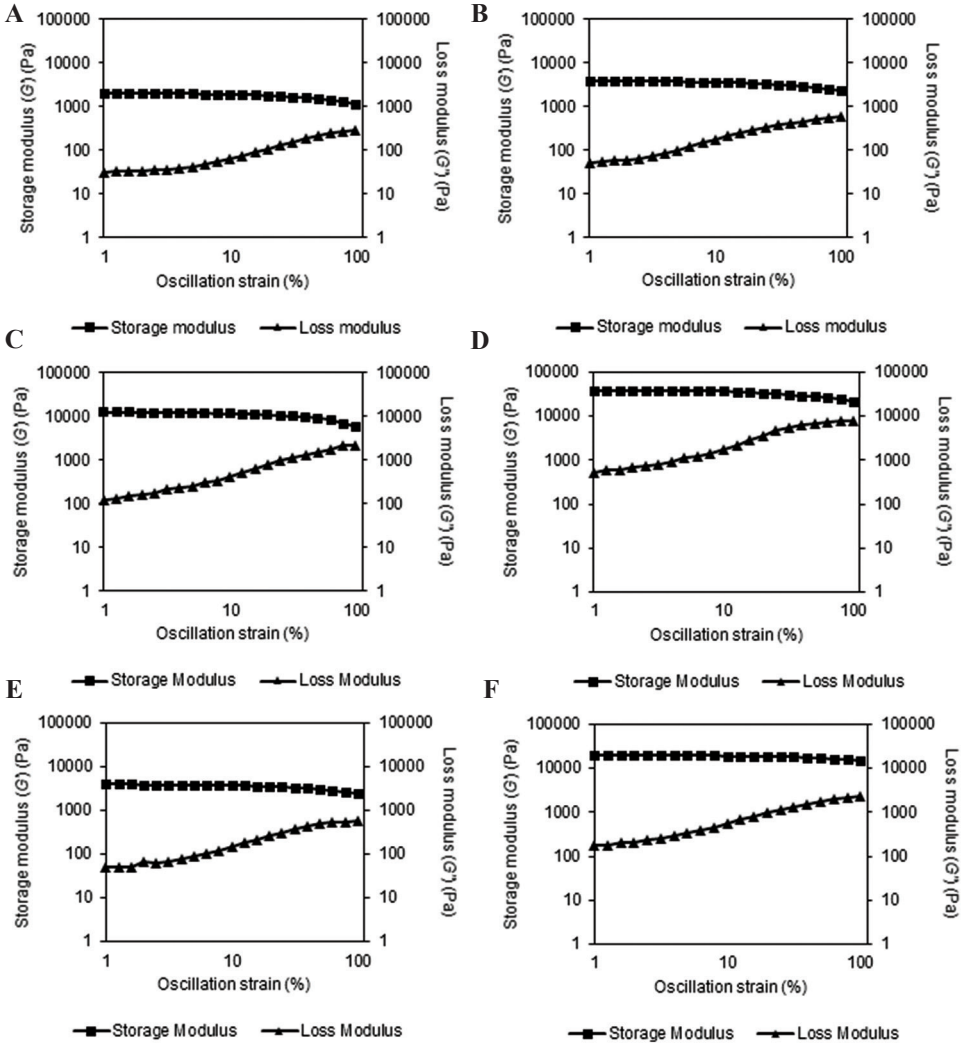

Figure 1. Flow diagrams of hydrogels made of different concentrations of FG and PG cross-linked with TG (5% w/w). (A) FG5. (B) FG7.5. (C) FG10. (D) FG20. (E) PG10. (F) PG20.

of under-gelation was the longest for PG10, which lasted at least 15 min (**Figure 2B**). The duration of proper-gelation was 5 min for FG7.5 and 20 min for PG10, respectively, while it was 2 min for FG10 (**Figure 2B**). Over-gelation was observed for FG7.5 and PG10 as the printed ink was clumpy and yielded the grids with irregular edges (**Figure 2A).** Over-gelation was also identified by a fractured grid morphology and disconnected filaments such as FG10 after 10 min. The gelation occurred most rapidly for FG10 among the three inks, where over-gelation manifested in a clogging nozzle and the filament barely extruded at the highest extrusion pressure (0.7 MPa). This clogging resulted in the inconsistent square grids with multiple broken interconnected filaments at 10 min, and the ink was hardly extruded at 15 min (**Figure 2A**). However, perfect squares may not be achieved even during proper gelation for every smaller square grid within the printed lattice. The discontinuity in the printed filament was due to a mismatch between the gelation state of the ink and the extrusion pressure. The ink became gradually gel-like in the nozzle with time due to crosslinking by TG. The increase in gelation required a corresponding increase in extrusion pressure to extrude the gel-like ink onto the substrate. However, as a single pressure was used to print the ink at every time point, small break

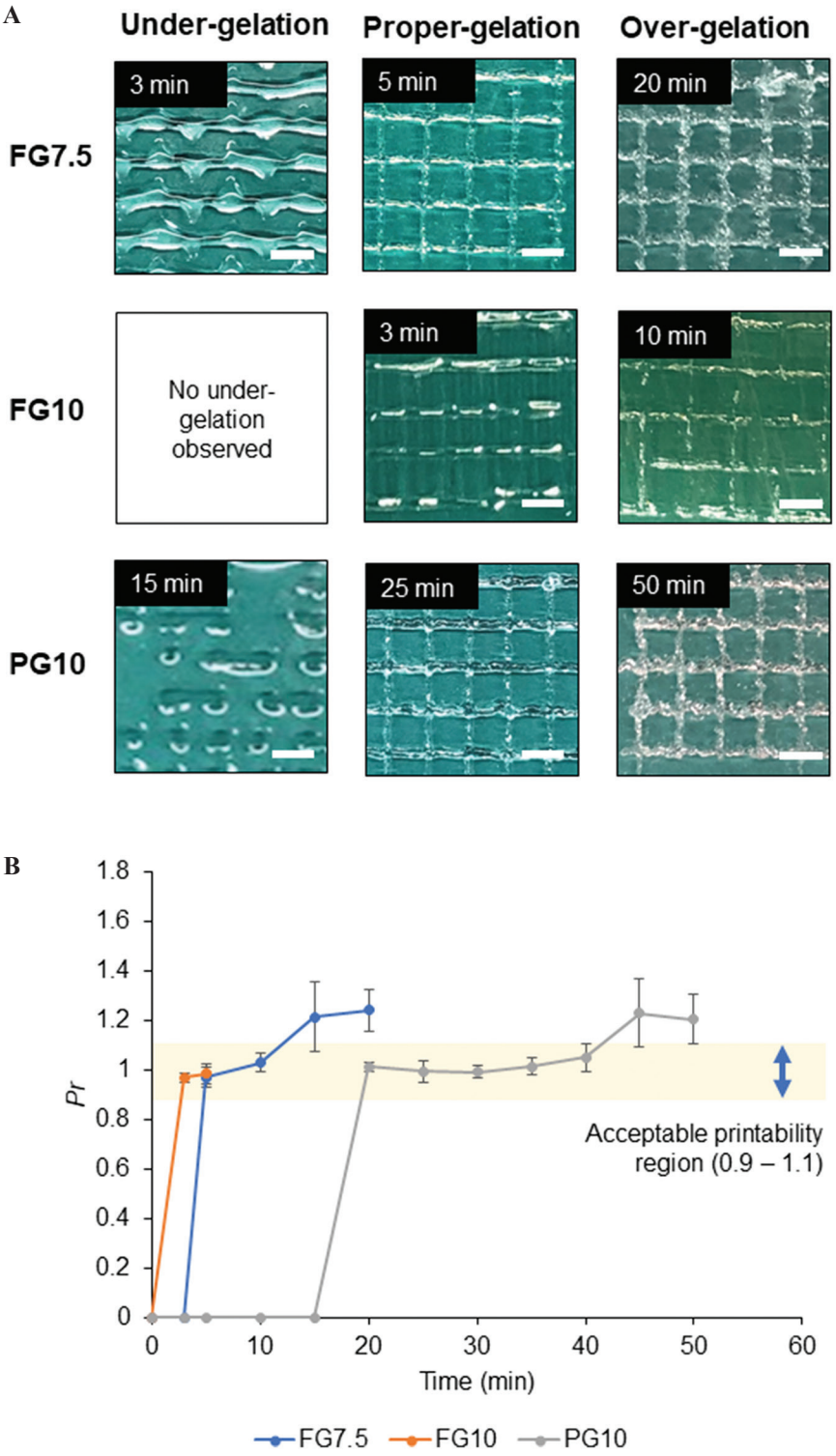

Figure 2. (A) Images of three-dimensional printed grid pattern using FG7.5, FG10, and PG10 each representing under-gelation, proper-gelation, and over-gelation, respectively. (Scale bar = 2.86 mm) (B) Evaluation of the duration of acceptable printability of the inks. The plot shows average *Pr* of the grid pattern at respective time points for FG7.5, FG10, and PG10.

(or discontinuity) could have occurred at specific points of the printed lattice. This error may not be critical due to the sufficiently large 3D printed lattice structure. We chose small square grids (n = 5) to calculate the average of Pr values at the respective time points. The values of Pr for FG7.5, FG10, and PG10 were plotted with respect to time to predict the duration for acceptable printability ($0.9 < Pr < 1.1$). Assuming linear changes in Pr between the data points, we estimated the duration of time that offered acceptable printability; the duration was the longest for PG10 (~20 min), which was higher than for FG7.5 (~5 min) and FG10 (~2 min) (**Figure 2B**).

2.4 Effect of PG ink on gelation time

The gelation of the ink triggered the phase change of the ink from liquid to gel due to enzymatic crosslinking. The viscosity of the ink became effectively infinite when the gelation completed[38].

The time point for the gelation allows us to approximate when the ink is printable with acceptable morphology and mechanical stability. We performed a time-sweep experiment to identify the gelation time of FG7.5, FG10, and PG10. The experiment was conducted at 40°C, which was consistent with the printing temperature of the inks. This temperature ensured that the gelation was solely due to enzymatic crosslinking but not due to the temperature at which the experiment was performed. The time point where the storage modulus matched with the loss modulus was recorded as the gelation time. Note that the reported values in this section include an extra 2.5 min (150 s) in addition to the time recorded by the rheometer (shown in the graphs in **Figure 3**). This extra time accounts for the time required to prepare the samples (i.e., mixing the gelatin with TG and loading it into the instrument). After the completion of the gelation, both storage and loss

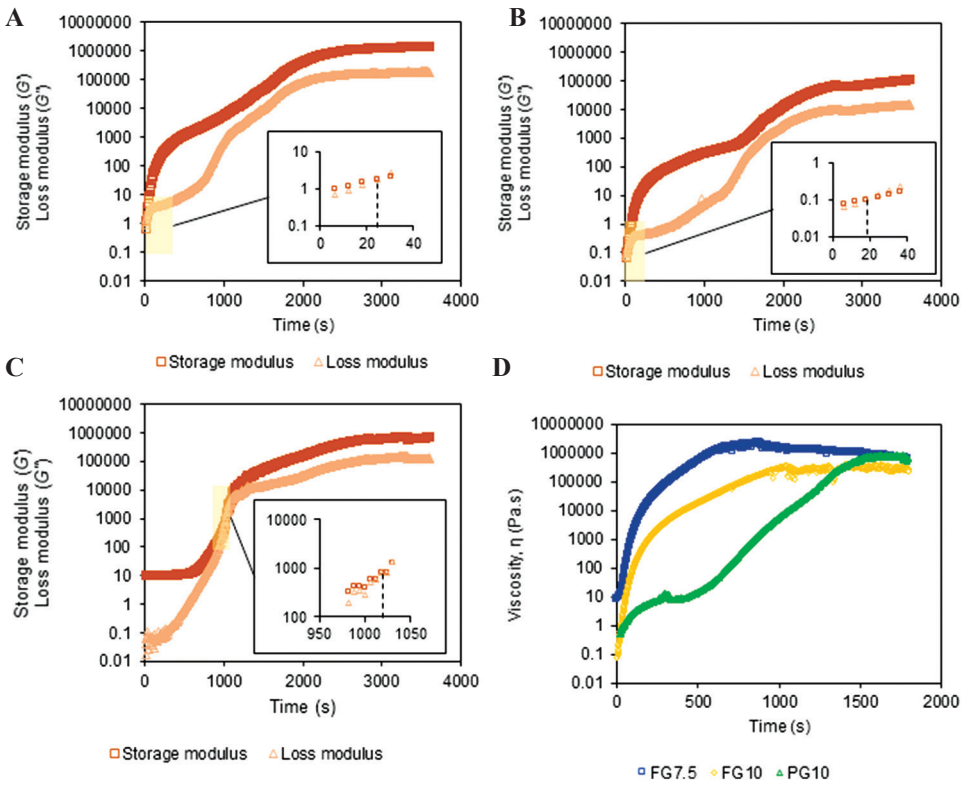

Figure 3. Rheological characterization of freshly prepared gelatin (FG7.5, FG10) and preheated gelatin (PG10). Time sweep tests indicating the storage modulus (G') and loss modulus (G'') of FG and PG at the respective concentrations: (A) FG7.5, (B), FG10, and (C) PG10. Regions of the curves were expanded to identify the gelation time point for each curve. (D) A plot showing the viscosity of FG7.5, FG10, and PG10 with time.

modulus reached a plateau. As observed with FG7.5 and FG10, the change in gelatin concentration had little effect on the gelation time for FG. However, the shorter gelation time in FG10 (~168 s) than FG7.5 (~174 s) may explain the mild spreading of FG7.5 ink at 3 min (**Figure 2A**), which was not apparent for FG10 (**Figure 2A**). PG10 exhibited the longest gelation time of 1169 s (19.4 min) (**Figure 3C**). This measurement was consistent with the spreading of PG10 ink at 20 min where proper-gelation was observed (**Figure 2B**).

2.5 Effect of preheating on ink viscosity

Viscosity is an essential parameter for extrusion-based printing as it determines the printability of the ink with a given pressure. A previous study has shown that the extrusion pressure is proportional to the zero-shear viscosity of the extruded filament[39]. The time-dependent change in the viscosity of the ink required us to control the extrusion pressure throughout the printing. We measured the viscosity of FG7.5, FG10, and PG10 over time (**Figure 3D**). The increase in the viscosity of FG and PG was due to the crosslinking of the gelatin by TG. The rate of increase in viscosity was evident by the gradient of the slope reflected in the viscosity-time curves, suggesting the required pressure to extrude the ink from the nozzle. The initial sharp increase in the viscosity of FG implied that the rapid increase in the extrusion pressure was required to ensure smooth printing. This rapid increase in the extrusion pressure resulted in somewhat unpredictable print quality with discontinuous or spread inks, which was observed for the FG inks (**Figure 3D**). The sharp increase in the viscosity for FG also explains the short duration of acceptable printability (**Figure 2B**) and rapid gelation (**Figure 3A, 3B**), both of which made the DIW 3D printing challenging for FG. In contrast, the increase in the viscosity occurred slower for PG10 than FG7.5 and FG10 (**Figure 3D**), allowing for relatively easy control over the printing pressure and smooth extrusion of the ink.

2.6 Swelling of hydrogels

The swelling test was performed on the hydrogels prepared from FG and PG. An isotonic environment was simulated with 1 × PBS, which would be an important consideration if the samples were used as cellular scaffolds. We studied the swelling of hydrogels by placing the hydrogel samples prepared from FG (FG7.5, FG10, and FG20) and PG (PG7.5, PG10, and PG20); all samples were crosslinked with TG (5% w/w) in 1 × PBS. The hydrogels were weighed at the beginning of the experiment and every 24 h post-soaking in 1 × PBS for 4 days. Their swelling ratios were plotted against the incubation time with 1 × PBS. (**Figure 4**)

For FG7.5, FG10, PG7.5, and PG10, a decrease in gel weights was observed post-soaking in 1 × PBS because 1 × PBS had a much higher ionic strength than the water contained in each gel. The gel placed in the hypertonic environment lost water due to the osmotic pressure. This effect surpassed the ability of hydrogels to absorb water, causing an overall decrease in the gel weights[26]. FG7.5 and FG10 showed a 20% reduction in gel weights after 24 h; the gel weights remained relatively constant up till 96 h subsequently. (**Figure 4**) In contrast, PG7.5 and PG10 exhibited up to 40% reduction in gel weights at 72 h, and remained relatively constant up till 96 h. At a high concentration of gelatin (i.e., FG20 and PG 20), we observed the swelling of the gel. FG20 showed 5% increase in gel weight after 24 h and remained relatively constant thereafter until 96 h. PG20 showed a 30%

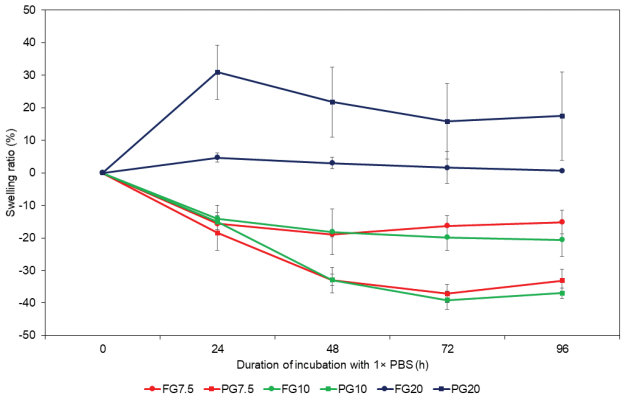

Figure 4. Swelling of the hydrogels. Changes in the swelling ratio for the respective FG and TG over 96 h incubation in 1× PBS. All samples of hydrogels contained 5% (w/w) of TG.

increase in gel weight after 24 h and equilibrated to a ~20% increase in gel weight until 96 h. The overall swelling could be attributed to a high concentration of gelatin (20%) in the hydrogel. Interestingly, FG exhibited smaller changes in gel weights than PG regardless of swelling or shrinking. This observation could be attributed to the rigidity of the gelatin network. Extended heating may cause the polypeptide chains of PG to be partially hydrolyzed. The resulting network in PG gel is more pliable than that in FG and may permit physical changes in the structure of the gel network. The flexibility of the gel network in PG allowed for an increased degree of shrinking or swelling in 1 × PBS, depending on the concentration of gelatin within the composition. Overall, the preheating of gelatin altered the properties to shrink or swell when placed in aqueous environments. The consideration of volume changes is essential when intending to create precise structures of gelatin by 3D printing. For the ink of PG10 that offered adequate printing duration, we shall account for the shrinkage if the printed model is used in aqueous environments.

3 Conclusions

In this paper, we explored the effect of preheating of gelatin to improve the duration of printable time in DIW 3D printing. Our study suggested that preheating gelatin for 7 days extended the duration of the acceptable printability 10 times longer than freshly prepared gelatin of the same concentration (10% w/w), and 4 times longer than freshly prepared gelatin with similar stiffness (10 kPa). The preheating of the gelatin altered the shrinking and swelling behaviors of the resulting hydrogels over 4 days in 1 × PBS, which provides an important consideration when the printed models are used in aqueous environments such as cell culture media. We believe the preheating of gelatin shall serve as a facile route to enhance the usability of gelatin in extrusion-based processes. Gelatin inks are increasingly used in DIW 3D printing to fabricate single-layered structures and multi-layered complex 3D structures that require a long duration of time for printing.

4 Materials and methods

4.1 Preparation of the inks and hydrogels

Freshly prepared gelatin (FG) was defined as gelatin (Porcine skin, Bloom 300, type A) (Sigma-Aldrich, USA) that had not undergone preheating. Briefly, FG stock was prepared by dissolving and mixing 12 g of gelatin powder with 18 g of distilled water in a water bath at 40 – 50°C with stirring until a clear yellow solution was obtained. Subsequently, the FG stock was kept at 4°C until further use. PG was prepared by placing an FG stock in a heat oven at 65°C for 7 days. Both gelatins were mixed with a 5% w/w TG (Moo Gloo TI TG) (Modernist Pantry, USA) to achieve their desired final concentrations before the experiments. To produce hydrogels, the final mixture was placed in the incubator at 37°C for 24 h to complete the crosslinking of gelatin by TG. The inks were prepared by mixing the gelatin stock solution that was pre-warmed to 40°C with TG. The mixture was subsequently stirred for 30 s before transferring into a metal syringe for printing. The addition of TG to gelatin initiated the gelation. The temperature of the ink was maintained in the syringe at 40°C throughout the printing.

4.2 DIW 3D printer and printability characterization

FG and PG inks were printed using a DIW 3D printer using a commercial 3D printing robot and a dispenser (SHOTmini 200 Sx and IMAGE MASTER 350 PC Smart, Musashi Engineering Inc., Japan). The dispenser was equipped with a single metal syringe (to maintain constant printing temperature) and a precise pressure controller (ML-5000XII and ML-808GX, Musashi Engineering Inc., Japan). MuCAD V software (Musashi Engineering Inc., Japan) was used to generate the design of the grid. Printing was performed with a metal nozzle head with a diameter of 200 μm under the dispending pressure ranging from 0.001 MPa to 0.7 MPa and the writing speed of 16 mm/s. The print speed was maintained at 16 mm/s to ensure the uniformity of

the printing condition for all printing. The printing temperature was at 40°C.

4.3 Assessment of the printability

FG7.5, FG10, and PG10 were prepared at 0 min. The inks were printed in a grid pattern on a glass surface at 3 min, 5 min, 10 min, and every 5 min after that. The printing was stopped when the inks became clumpy or when the ink could not be extruded at the maximum pressure of the dispenser. The value of *Pr* was calculated from the printed grid pattern of the inks at respective time points. The entire printed grid pattern was a square measuring 2 cm by 2 cm, with a size of 4 cm^2. Briefly, *Pr* was calculated from the perimeter (*L*) and area (*A*) of each square shape ($n = 5$) within the printed grid pattern formed by the interconnected filaments using the formula: $Pr = L^2/16A$[36]. Optical images of the printed constructs were analyzed to determine the L and A of the interconnected filaments. All image processing was done using ImageJ software[40].

4.4 Rheological analysis of gelatin and TG ink

Rheometer (Discovery HR-2, TA Instruments, USA) with a 20 mm parallel plate was used to measure the gel storage modulus (*G'*), loss modulus (*G"*), gelation time, and viscosity for the various compositions of FG and PG samples at 40°C. *G'* and *G"* were determined by the oscillatory stress sweep test at a constant angular frequency of 10 rad s^{-1} with a logarithmic shear strain ramp from 1% to 100%. Gelation time was measured at 1% oscillation strain and 1 Hz frequency. Viscosity testing was performed at a constant shear rate of 0.01 s^{-1}.

4.5 Gel swelling

10 g of the gel solutions containing respective final concentrations of FG and PG were poured into a Petri dish (90 mm × 15 mm) and incubated at 37°C for 24 h to allow complete crosslinking of the gelatin chains. Subsequently, a square acrylic mold (20 mm × 20 mm × 2 mm) prepared from laser cutting was pressed into the hydrogel to create square pieces of the samples at 600 mg each. Each piece of hydrogel prepared from respective concentrations of FG or PG was placed into a Petri dish (30 mm × 15 mm) and incubated with 1 × PBS (Nacalai Tesque, Japan) for 4 days. The hydrogels were weighed before soaking in the media, and every 24 h up post-soaking until Day 4 ($n = 3$). The swelling ratio was calculated from the following equation:

$$Swelling\ ratio = \frac{W_t - W_o}{W_o} \times 100$$

where W_t was the weight of the swollen sample at the respective time point and W_o was the initial weight of the sample.

Acknowledgments

The authors would like to thank International Design Centre at Singapore University of Technology and Design (SUTD) (IDG11700103) and Agency for Science, Technology and Research (A*STAR) (A19B9b0067) for the project support. The authors thank the members of Hashimoto Group at SUTD for helpful feedback.

Conflicts of interest

The authors declare that they have no conflicts of interest.

Authors' contributions

J.J.Y.T., C.P.L., and M.H. planned the experiment. J.J.Y.T. and C.P.L. carried out the experiments. M.H. supervised the experiments. J.J.Y.T. and M.H. wrote the paper.

References

1. Ng WL, Chua CK, Shen YF, 2019, Print me an Organ! Why we are not there yet. *Prog. Polym. Sci*, 2019:101145. DOI: 10.1016/j.progpolymsci.2019.101145.
2. Lee JM, Ng WL, Yeong WY, 2019, Resolution and Shape in Bioprinting: Strategizing Towards Complex Tissue and Organ Printing. *Appl Phys Rev*, 6:011307. DOI: 10.1063/1.5053909.
3. Guo SZ, Qiu K, Meng F, *et al.*, 2017, 3D printed stretchable tactile sensors. *Adv Mater*, 29:1701218. DOI: 10.1002/adma.201701218.
4. Voon SL, An J, Wong G, *et al.*, 2019, 3D Food Printing: A

Categorised Review of Inks and their Development. *Virtual Phys Prototyp*, 14:203–18.

5. Karyappa R, Hashimoto M, 2019, Chocolate-based Ink Three-dimensional Printing (Ci3DP). *Sci Rep*, 9:1–11. DOI: 10.1038/s41598-019-50583-5.
6. Gariboldi MI, Best SM, 2015, Effect of Ceramic Scaffold Architectural Parameters on Biological Response. *Front Bioeng Biotech*, 3:151. DOI: 10.3389/fbioe.2015.00151.
7. Sun H, Zhu F, Hu Q, *et al.*, 2014, Controlling Stem Cell-mediated Bone Regeneration Through Tailored Mechanical Properties of Collagen Scaffolds. *Biomaterials*, 35:1176–84. DOI: 10.1016/j.biomaterials.2013.10.054.
8. Kuttappan S, Mathew D, Nair MB, 2016, Biomimetic Composite Scaffolds Containing Bioceramics and Collagen/ Gelatin for Bone Tissue Engineering a Mini Review. *Int J Biol Macromol*, 93:1390–401. DOI: 10.1016/j.ijbiomac.2016.06.043.
9. Irvine SA, Agrawal A, Lee BH, *et al.*, 2015, Printing Cell-laden Gelatin Constructs by Free-form Fabrication and Enzymatic Protein Crosslinking. *Biomed Microdevices*, 17:16. DOI: 10.1007/s10544-014-9915-8.
10. Bettadapur A, Suh GC, Geisse NA, *et al.*, 2016, Prolonged Culture of Aligned Skeletal Myotubes on Micromolded Gelatin Hydrogels. *Sci Rep*, 6:28855. DOI: 10.1038/srep28855.
11. Osorio FA, Bilbao E, Bustos R, *et al.*, 2007, Effects of Concentration, Bloom Degree, and pH on Gelatin Melting and Gelling Temperatures Using Small Amplitude Oscillatory Rheology. *Int J Food Prop*, 10:841–51. DOI: 10.1080/10942910601128895.
12. Pepelanova I, Kruppa K, Scheper T, *et al.*, 2018, Gelatin-Methacryloyl (GelMA) Hydrogels with Defined Degree of Functionalization as a Versatile Toolkit for 3D Cell Culture and Extrusion Bioprinting. *Bioengineering* (*Basel*), 5:55. DOI: 10.3390/bioengineering5030055.
13. Karyappa R, Ching T, Hashimoto M, 2020, Embedded Ink Writing (EIW) of Polysiloxane Inks. *ACS Appl Mater Inter*, 12:23565–75. DOI: 10.1021/acsami.0c03011.
14. Karyappa R, Ohno A, Hashimoto M, 2019, Immersion Precipitation 3D Printing (ip 3DP). *Mater Horiz*, 6:1834–44. DOI: 10.1039/c9mh00730j.
15. Melocchi A, Parietti F, Maroni A, *et al.*, 2016, Hot-melt Extruded Filaments Based on Pharmaceutical Grade Polymers for 3D Printing by Fused Deposition Modeling. *Int J Pharm*, 509:255–63. DOI: 10.1016/j.ijpharm.2016.05.036.
16. Ghazal AF, Zhang M, Liu Z, 2019, Spontaneous Color Change of 3D Printed Healthy Food Product over Time after Printing as a Novel Application for 4D Food Printing. *Food Bioproc Tech.*, 12:1627–45. DOI: 10.1007/s11947-019-02327-6.
17. Dhariwala B, Hunt E, Boland T, 2004, Rapid Prototyping of Tissue-engineering Constructs, Using Photopolymerizable Hydrogels and Stereolithography. *Tissue Eng*, 10:1316–22. DOI: 10.1089/1076327042500256.
18. Skardal A, Zhang J, McCoard L, *et al.*, 2010, Photocrosslinkable Hyaluronan-gelatin Hydrogels for Two-step Bioprinting. *Tissue Eng Part A*, 16:2675–85. DOI: 10.1089/ten.tea.2009.0798.
19. Billiet T, Gevaert E, De Schryver T, *et al.*, 2014, The 3D Printing of Gelatin Methacrylamide Cell-laden Tissue-engineered Constructs with High Cell Viability. *Biomaterials*, 35: 49–62. DOI: 10.1016/j.biomaterials.2013.09.078.
20. Duan B, Hockaday LA, Kang KH, *et al.*, 2013, 3D Bioprinting of Heterogeneous Aortic Valve Conduits with Alginate/ Gelatin Hydrogels. *J Biomed Mater ResA*, 101:1255–64. DOI: 10.1002/jbm.a.34420.
21. Kirchmajer DM, Iii RG, 2015, An Overview of the Suitability of Hydrogel-forming Polymers for Extrusion-based 3D-printing. *J Mater Chem B*, 3:4105–17. DOI: 10.1039/c5tb00393h.
22. Chang R, Nam J, Sun W, 2008, Effects of Dispensing Pressure and Nozzle Diameter on Cell Survival from Solid Freeform Fabrication Based Direct Cell Writing. *Tissue Eng Part A*, 14:41–8. DOI: 10.1089/ten.2007.0004.
23. Mondal MI, 2019, Cellulose-Based Superabsorbent Hydrogels. Springer, Berlin, Germany.
24. Tice L, Moore A, 1952, Heat Denatured Gelatin. *J Am Pharm Assoc*, 41:631–3.
25. Qi J, Zhang WW, Feng XC, *et al.*, 2018, Thermal Degradation of Gelatin Enhances its Ability to Bind Aroma Compounds: Investigation of Underlying Mechanisms. *Food Hydrocoll*, 83:497–510. DOI: 10.1016/j.foodhyd.2018.03.021.
26. Xing Q, Yates K, Vogt C, *et al.*, 2014, Increasing Mechanical Strength of Gelatin Hydrogels by Divalent Metal Ion Removal. *Sci Rep*, 4:4706. DOI: 10.1038/srep04706.
27. Janmey PA, Miller RT, 2011, Mechanisms of Mechanical Signaling in Development and Disease. *J Cell Sci*, 124:9–18.
28. Solon J, Levental I, Sengupta K, *et al.*, 2007, Fibroblast Adaptation and Stiffness Matching to Soft Elastic Substrates. *Biophys J*, 93:4453–61. DOI: 10.1529/biophysj.106.101386.
29. Mogha P, Srivastava A, Kumar S, *et al.*, 2019, Hydrogel Scaffold with Substrate Elasticity Mimicking Physiological-niche Promotes Proliferation of Functional Keratinocytes. *RSC Adv*, 9:10174–83. DOI: 10.1039/c9ra00781d.
30. Chan SW, Rizwan M, Yim EK, 2020, Emerging Methods for

Enhancing Pluripotent Stem Cell Expansion. *Front Cell Dev Biol*, 8:70. DOI: 10.3389/fcell.2020.00070.

31. Tan JJ, Tee JK, Chou KO, *et al.*, 2018, Impact of Substrate Stiffness on Dermal Papilla Aggregates in Microgels. *Biomater Sci*, 6:1347–57.
32. Croome R, 1959, The Rapid Formation and Breakdown of Gelatin Gels, and the Temperature-dependence of their Rigidity. *J Sci Food Agric*, 10:394–400. DOI: 10.1002/jsfa.2740100708.
33. Gerardo H, Lima A, Carvalho J, *et al.*, 2019, Soft Culture Substrates Favor Stem-like Cellular Phenotype and Facilitate Reprogramming of Human Mesenchymal Stem/Stromal Cells (hMSCs) through Mechanotransduction. *Sci Rep*, 9:1–18. DOI: 10.1038/s41598-019-45352-3.
34. Kureel SK, Mogha P, Khadpekar A, *et al.*, 2019, Soft Substrate Maintains Proliferative and Adipogenic Differentiation Potential of Human Mesenchymal Stem Cells on Long-term Expansion by Delaying Senescence. *Biol Open*, 8:bio039453. DOI: 10.1101/364059.
35. Gilbert PM, Havenstrite KL, Magnusson KE, *et al.*, 2010, Substrate Elasticity Regulates Skeletal Muscle Stem Cell Self-renewal in Culture. *Science*, 329:1078–81. DOI: 10.1126/science.1191035.
36. Ouyang L, Yao R, Zhao Y, *et al.*, 2016, Effect of Bioink Properties on Printability and Cell Viability for 3D Bioplotting of Embryonic Stem Cells. *Biofabrication*, 8:035020. DOI: 10.1088/1758-5090/8/3/035020.
37. Nauenberg M, 2014, A Paradox with the Hagen-Poiseuille Relation for Viscous Fluid Flow. *Am J Phys*, 82:82–5. DOI: 10.1119/1.4825138.
38. Mulder M, 2000, Membrane preparation. In: Encyclopedia of Separation Science: Phase Inversion Membranes. Elsevier, Amsterdam, Netherlands, pp. 3331–3346. DOI: 10.1016/b0-12-226770-2/05271-6.
39. Zhu S, Stieger MA, van der Goot AJ, *et al.*, 2019, Extrusion-based 3D Printing of Food Pastes: Correlating Rheological Properties with Printing Behaviour. *Innov Food Sci Emerg*, 58:102214. DOI: 10.1016/j.ifset.2019.102214.
40. Schneider CA, Rasband WS, Eliceiri KW, 2012, NIH Image to ImageJ: 25 Years of Image Analysis. *Nat Methods*, 9:671–5. DOI: 10.1038/nmeth.2089.